INVESTIGATION OF LATE QUATERNARY FAULT SCARPS ALONG THE BITTERROOT FAULT IN WESTERN MONTANA

Michael C. Stickney and Jeffrey D. Lonn

2018

MBMG

Montana Bureau of Mines and Geology

Cover photo by Jeffery Lonn, MBMG. Southward view of the Bitterroot Fault offsetting the late Quaternary Ward Creek alluvial fan.

Investigation of Late Quaternary Fault Scarps along the Bitterroot Fault in Western Montana

Michael C. Stickney and Jeffrey D. Lonn

Montana Bureau of Mines and Geology

MBMG Report of Investigation 24

2018

TABLE OF CONTENTS

FIGURES

PLATES

ABSTRACT

We used a high-resolution digital elevation model created from LiDAR data as a base for constructing detailed geologic maps for two areas along the Bitterroot Range front where the Bitterroot Fault offsets a variety of Quaternary deposits. Faults offset post-glacial outwash surfaces and glacial till interpreted to be late Pinedale age by as much as 2 m. Deposits and geomorphic surfaces that we interpret as early Pinedale age and older have fault offsets from 8 to 11 m. Debris flow-mantled pediment surfaces of older, but unknown, age have fault offsets ranging up to 43 m. Lacking age control for the faulted deposits and surfaces, we cannot yet estimate fault slip rates; however, progressively larger fault offsets of older deposits and surfaces demonstrate that repeated surface-rupturing earthquakes have occurred along the Bitterroot Fault during the latest Pleistocene. This finding suggests that the Quaternary Fault and Fold Database and the National Seismic Hazard Maps may underestimate the true seismic hazard level of the Bitterroot Fault.

INTRODUCTION

The Bitterroot Fault is a 100-km-long east-dipping normal fault in western Montana that bounds the eastern side of the north–south-trending Bitterroot Range (fig. 1). The USGS Quaternary Fault and Fold Database lists the Bitterroot Fault, but contains minimal data with which to characterize the fault—a default slip rate of <0.2 mm/year and the most recent event younger than 1.6 million years. Thus, the Bitterroot Fault is not included in the preparation of the National Seismic Hazard Maps, despite its proximity to over 150,000 residents in the adjacent Bitterroot and Missoula Valleys. Although the National Seismic Hazard Maps identify western Montana as a region of high seismic hazard, coinciding with the northern part of the Intermountain Seismic Belt and the Centennial Tectonic Belt (fig. 2), the maps show the Bitterroot Valley as the region of lowest seismic hazard in western Montana. However, newly available LiDAR data that covers most of the Bitterroot Valley reveals late Quaternary scarps along the Bitterroot Fault.

LiDAR data analysis is a valuable tool for identifying previously unrecognized Pleistocene fault scarps and for evaluating fault characteristics and associated hazards (e.g., Hunter and others, 2011; Thackray and others, 2013; Thackray and Staley, 2017). In this study, we use LiDAR data in conjunction with new field mapping to examine the extent and character of Quaternary offset along the Bitterroot Fault in two areas where fault scarps cut Quaternary landforms of several ages. U.S. Geological Survey Earthquake Hazards Program grant G17AP00051 partly funded this project.

METHODS

In this study, we mapped two areas in detail (fig. 1) where bare earth images created from LiDAR data showed fault scarps offsetting late Pleistocene deposits and surfaces. The northern Bitterroot map (plate 1; scale 1:24,000) covers about 100 km^2 surrounding the Poverty Flat and Big Creek scarps near Victor. The southern Bitterroot map (plate 2, scale 1:12,000) encompasses about 35 km^2 surrounding the Lost Horse and Ward Creek scarps southwest of Hamilton. Using the LiDAR data, we drew topographic profiles across the scarps to measure vertical surface offsets and scarp heights, and compared them across the various map units. Because no absolute age data are yet available for the geomorphic surfaces or Quaternary map units, we conducted a literature review to estimate tentative ages based on previous studies of glacial history in surrounding regions.

PREVIOUS WORK AND GEOLOGIC SETTING

Small-scale maps by Ross (1952), Toth (1983), McMurtrey and others (1972), Berg and Lonn (1996), Lonn and Berg (1996), and Lonn and Sears (2001) cover both bedrock and surficial geology of the region. Weber (1972) studied the glacial history of the valley, and Barkman (1984) and Cartier (1984) addressed the question of active tectonism in the Bitterroot Valley. Lonn and Sears (2001) show an index map of previous mapping in the region.

The Bitterroot Fault runs for 100 km along the eastern base of the Bitterroot Mountains (U.S. Geo-
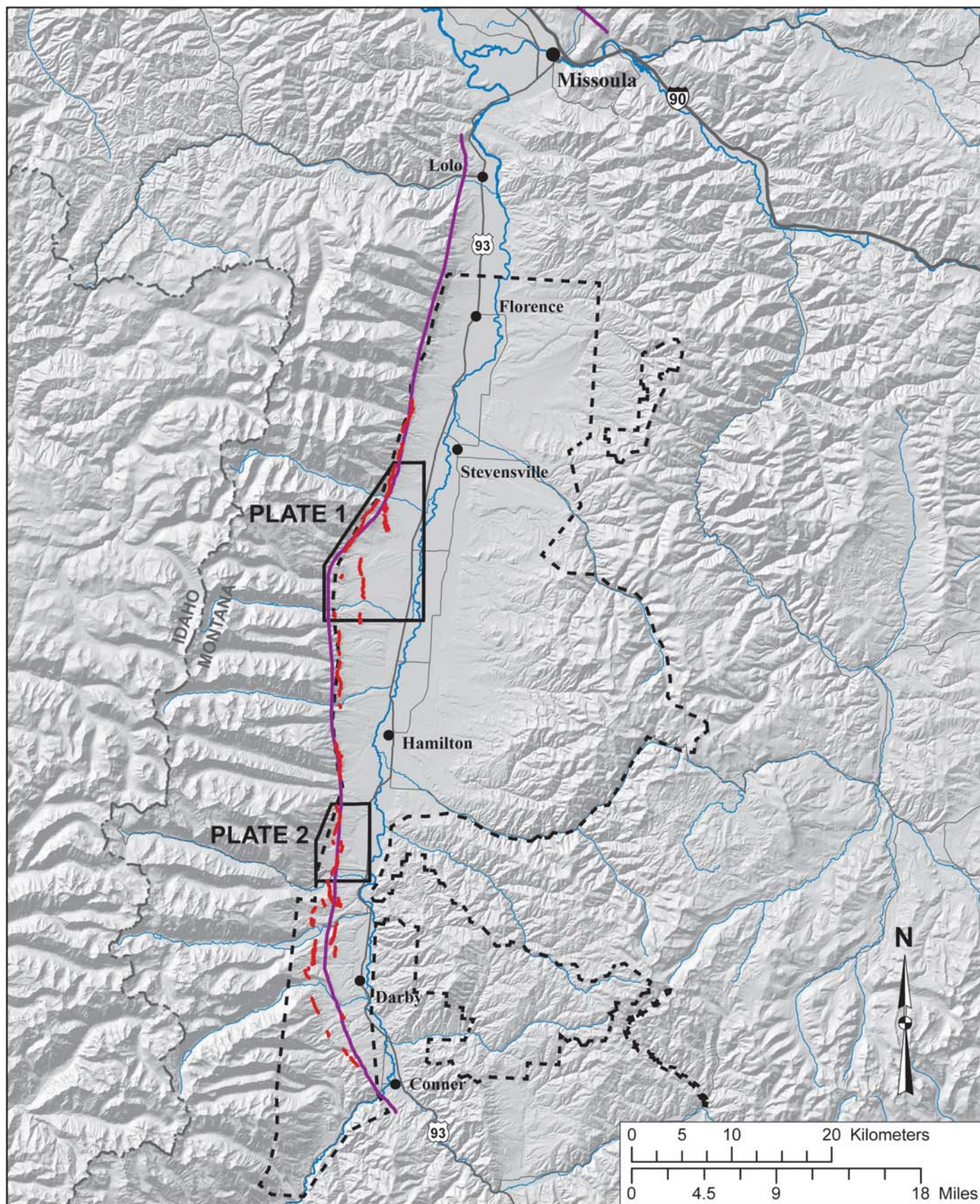
Figure 1. Topographic map showing the Bitterroot Valley and Bitterroot Range to the west. Violet line shows the Bitterroot Fault from the USGS Quaternary Fault and Fold database. Red line segments indicate late Quaternary fault scarps identified on bare earth image derived from LiDAR data. Dashed black line shows the extent of the LiDAR coverage. Black polygons southwest of Stevensville and south of Hamilton show the extent of detailed mapping for the northern and southern map areas, respectively.
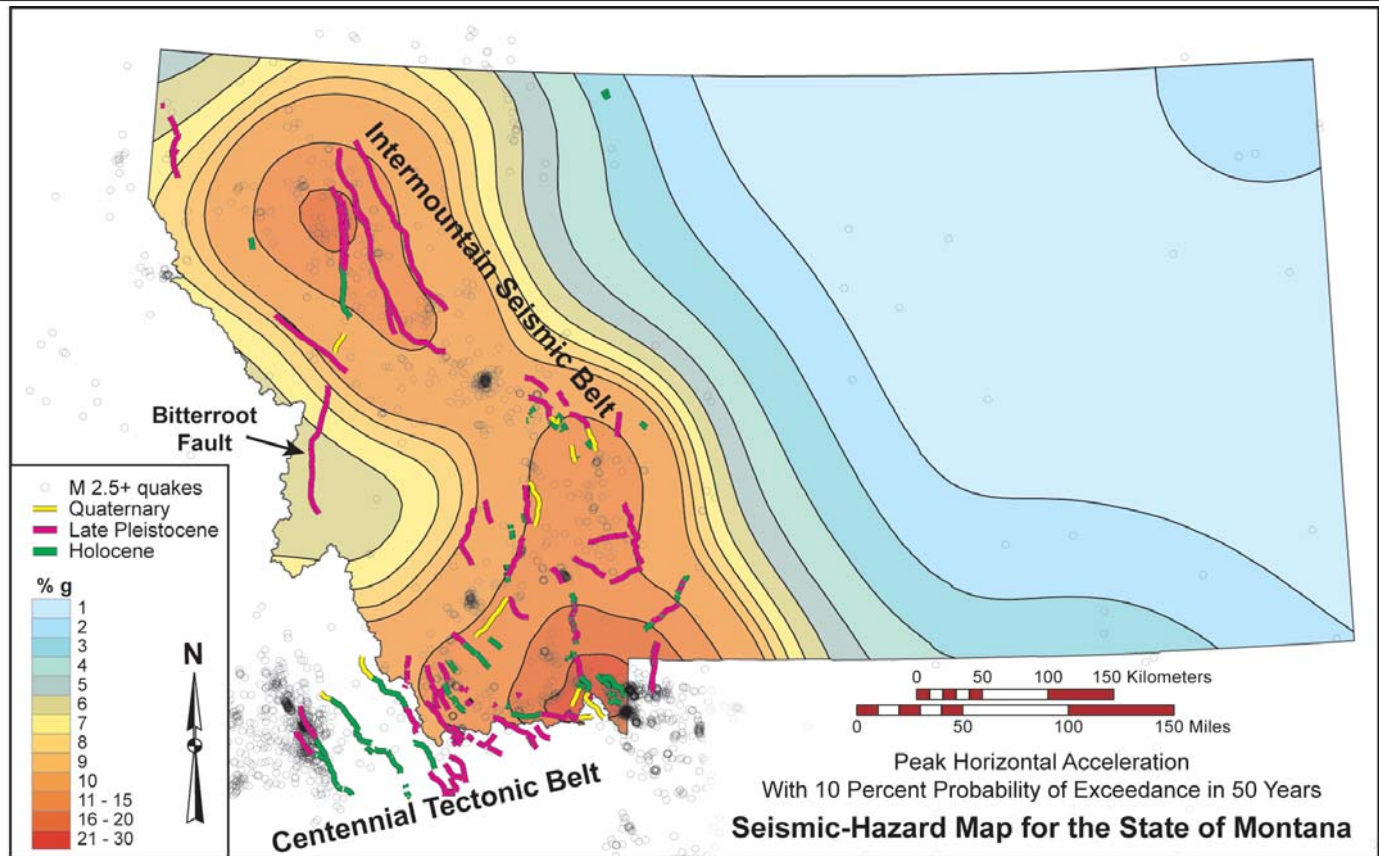
Source and Reference Material: USGS - http://pubs.usgs.gov/sim/2005/2883/pdf/2883-1.pdf

Figure 2. Montana seismic hazard map, Quaternary faults, and circles showing earthquakes with magnitudes of 2.5 or larger since 1982.

logical Survey and Montana Bureau of Mines and Geology, 2006) that constitute the metamorphic infrastructure of a well-studied Eocene metamorphic core complex (e.g., Hyndman, 1980; Foster and others, 2001). Previous maps show discontinuous segments of the Bitterroot fault (Berg and Lonn, 1996; Lonn and Berg, 1996; Lonn and Sears, 2001) as steeply east-dipping faults cutting the more gently dipping Eocene Bitterroot detachment (referred to herein as the "B-detachment" to avoid confusion with the Quaternary Bitterroot Fault that is the focus of this study). Foster and Raza (2002) postulated that the steep-dipping, normal Bitterroot Fault was Miocene in age and responsible for the uplift and exposure of the older Eocene B-detachment fault (fig. 3). However, Barkman (1984) and Cartier (1984) proposed that faults are active in the Bitterroot Valley, and Lonn and Sears (2001) included Barkman's (1984) fault scarps on their surficial geologic map. Some of those scarps partly coincide with scarps revealed by the LiDAR analysis.

Cretaceous–Early Tertiary Geologic History

Cretaceous to Eocene intrusive rocks and less common Mesoproterozoic metasedimentary rocks and Paleoproterozoic metamorphic rocks underlie the Bitterroot Mountains in the footwall of the 53–30 Ma B-detachment (Foster and Raza, 2002). The gently east-dipping B-detachment (fig. 3) was responsible for the rapid exhumation of these mid-crustal rocks from depths of >20 km (Foster and others, 2001). This fault exhibits a transition from amphibolite facies mylonitization to greenschist facies shearing to brittle faulting through time as structural levels became increasingly shallow.

The hanging wall of the B-detachment is comprised mainly of Mesoproterozoic metasedimentary rocks with lesser Cretaceous to Eocene granitic rocks and Paleoproterozoic metamorphic rocks. In the few places where these rocks are preserved near the B-detachment along the Bitterroot front, they are ex-

3

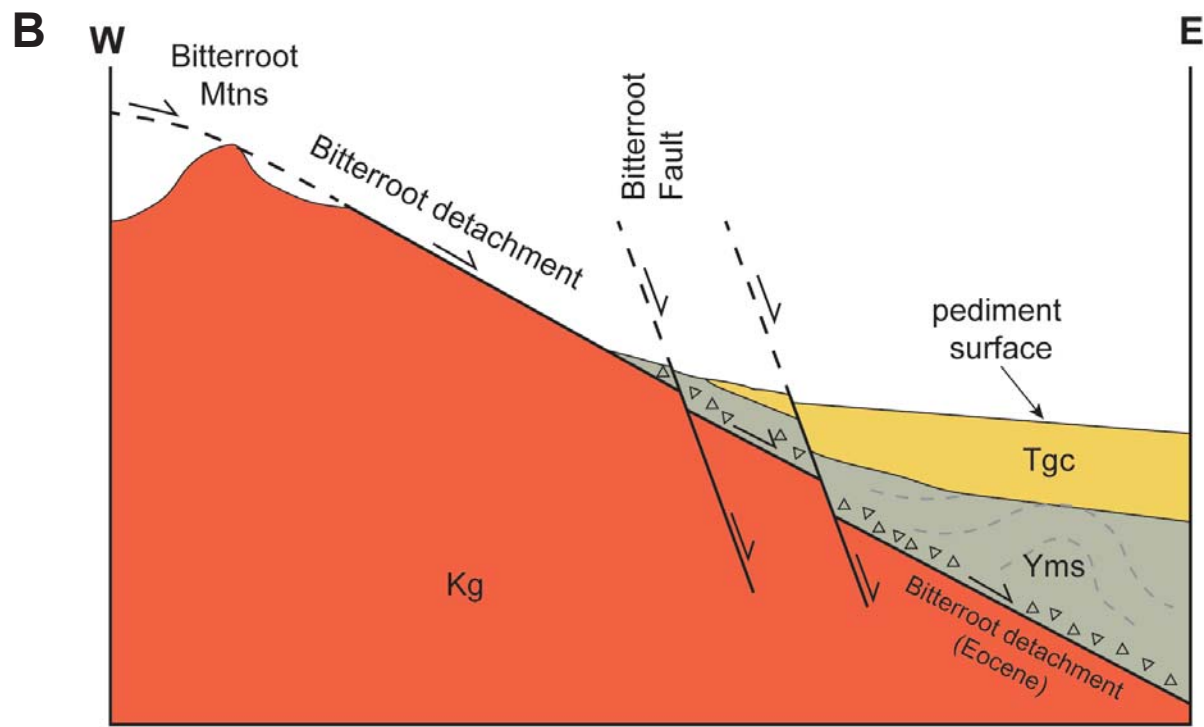Figure 3. (A) Northwestward view of the eastern Bitterroot Range front. Flatirons are resistant mylonitic gneiss that defines the Eocene Bitterroot detachment fault. The Quaternary Bitterroot Fault extends along the base of the mountains. (B) Cross section sketch showing relationships between the Eocene detachment and the cross-cutting Quaternary Bitterroot normal fault, confirmed by geologic mapping in this study.

tensively brecciated, in contrast to the gneissic and mylonitized footwall rocks. On plates 1 and 2, the trace of the B-detachment Fault is shown approximately at the contact between the amphibolite facies mylonite, shown by mylonitic foliation and lineation symbols, and the brecciated rocks. The trace of the B-detachment is exposed on pediment surfaces east of the mountain front in the southern map area (plate 2) and exposed discontinuously along the mountain front in the northern map area (plate 1).

By about 26 Ma (Foster and Raza, 2002), the steeply east-dipping normal faults became active, offsetting the B-detachment (fig. 3B). The active Bitterroot Fault is the modern expression of this Basin-and-Range-style normal fault. Stickney and Bartholomew (1987) and Lageson and Stickney (2000) attribute other western Montana mountain ranges lacking metamorphic core complexes, but bounded by late Quaternary normal faulting, to east–west or northeast–southwest extension in the northern Basin and Range province. The Bitterroot Fault uplifted the resistant gneiss of the B-detachment Fault footwall, and the present topographic expression of the Bitterroot Mountains and Valley is attributed to this gneiss zone. West of the Bitterroot Fault, erosion removed most of the brecciated and less resistant rocks of the B-detachment hanging wall, leaving the resistant gneiss of the footwall to form the planar, gently sloping Bitterroot Mountain front (fig. 3A).

Mapping Results: Late Tertiary–Quaternary Geologic History

As Basin and Range faulting along the Bitterroot Fault uplifted the mountains and deepened and widened the Bitterroot Valley, unconsolidated Cenozoic deposits accumulated in the valley to depths as much as 730 m (Norbeck, 1980). The oldest unconsolidated Cenozoic deposits exposed in the map areas are Oligocene to Pliocene(?) (McMurtrey and others, 1972) Tgc and Tgcd. Unit Tgc consists of sandy, well-sorted, pebble–cobble conglomerate containing rounded clasts dominantly of Belt quartzite, but also including lesser granitic mylonite, volcanic rocks, and metamorphic rocks. These gravels are interbedded with tuffaceous silt and clay intervals. Because the clasts are derived from lithologies present in the entire Bitterroot River basin, Lonn and Sears (2001) interpreted Tgc as a fluvial deposit deposited by an ancestral Bitterroot

River (McMurtrey and others, 1972). Near the Bitterroot Mountain front, unit Tgcd consists mainly of sub-angular boulders and cobbles of Belt quartzite and quartzite breccia similar to the bedrock exposed immediately above the B-detachment. Tgcd interfingers with Tgc and are interpreted as debris flow deposits marginal to the ancestral valley. Clast compositions of these deposits predominately represent lithologies of the hanging wall of the B-detachment Fault and suggest that the granitic core of the metamorphic complex remained largely unexposed at the time of their deposition. The lower contact of Tgc is exposed at two places on the southern Bitterroot map (plate 2), where it lies on top of brecciated granitic bedrock. The upper Tgc contact is a pediment surface with a minimum age constrained only by the overlying Pleistocene glacial deposits.

Older glacial outwash deposits (units Qgoo, Qgdo) mantle these relict pediment surfaces and are associated with older till (Qgto) deposited at high levels downstream from the mouths of the Bitterroot Mountain canyons. Weber (1972) postulated that these older glacial deposits represent at least two different glacial stages, but we could not distinguish them in the field or on the LiDAR image. However, in the northern map area we identified an intermediate level of outwash in the Poverty Flat area.

Younger glacial deposits (Qgom, Qgoy, Qgty) occur between and topographically below incised remnants of the older deposits. The youngest post-glacial Holocene fluvial and alluvial deposits (Qal) are associated with modern stream floodplains and occur at the lowest topographic levels, incised into all Pleistocene glacial deposits.

The fieldwork and LiDAR data analysis show that fault scarps cut surfaces of at least three different ages, with increasing offset on surfaces of increasing age. Although important to the determination of slip rate and earthquake recurrence intervals, no absolute age data are yet available for the Quaternary deposits or surfaces. The field mapping also shows that the Bitterroot Fault cuts both the hanging wall and footwall of the B-detachment, indicating that the Bitterroot Fault is indeed a steep fault as shown in figure 3B, and does not sole into the more gently dipping B-detachment.

LIDAR ANALYSIS: FAULT OFFSET OF GEOLOGIC UNITS AND FEATURES, NORTH BITTERROOT MAP

With a relative median accuracy of 4 cm (5 cm two sigma relative accuracy), the bare-earth digital elevation model (DEM) produced from the Bitterroot Valley LiDAR data provides very detailed images of the earth's surface. We used this DEM to produce a detailed hillshade image on which we mapped surficial geologic deposits and the faults that offset them in selected areas along the western side of the Bitterroot Valley. We also used the DEM together with ArcMap v. 10.5.1 software to generate 12 topographic profiles across fault scarps. We selected sites for topographic profiling where a geomorphic surface showed distinct offset across the fault. The original LIDAR data have elevations measured in feet but distances in meters, hence the mixture of English and metric units on the topographic profiles.

Plate 1 shows the geology of the northern map area. The northernmost topographic profile (fig. 4, A–A') is located on an alluvial terrace about 125 m south of and parallel to Big Creek. This terrace formed immediately below the mouth of the bedrock canyon from which Big Creek issues from the Bitterroot Mountains. We mapped glacial till near the mouth of Big Creek Canyon, but the glacier apparently did not extend beyond the canyon mouth into the Bitterroot Valley. We interpret the low terrace (mapped as Qgoy) that flanks Big Creek as a glacial outwash terrace that formed during the most recent deglaciation, which we assume is latest Pinedale. Evidence for the youthful nature of this terrace is its position adjacent to the modern stream channel, which is incised 3–4 m into this surface, and bar and swale morphology clearly visible on the DEM. Below the fault scarp, the terrace surface slopes 1.5° eastward. The topographic profile indicates 1.7 m of offset on this surface across the Bitterroot Fault. We see no evidence for fault offset in the modern stream channel. Fault offset of 1.7 m on this
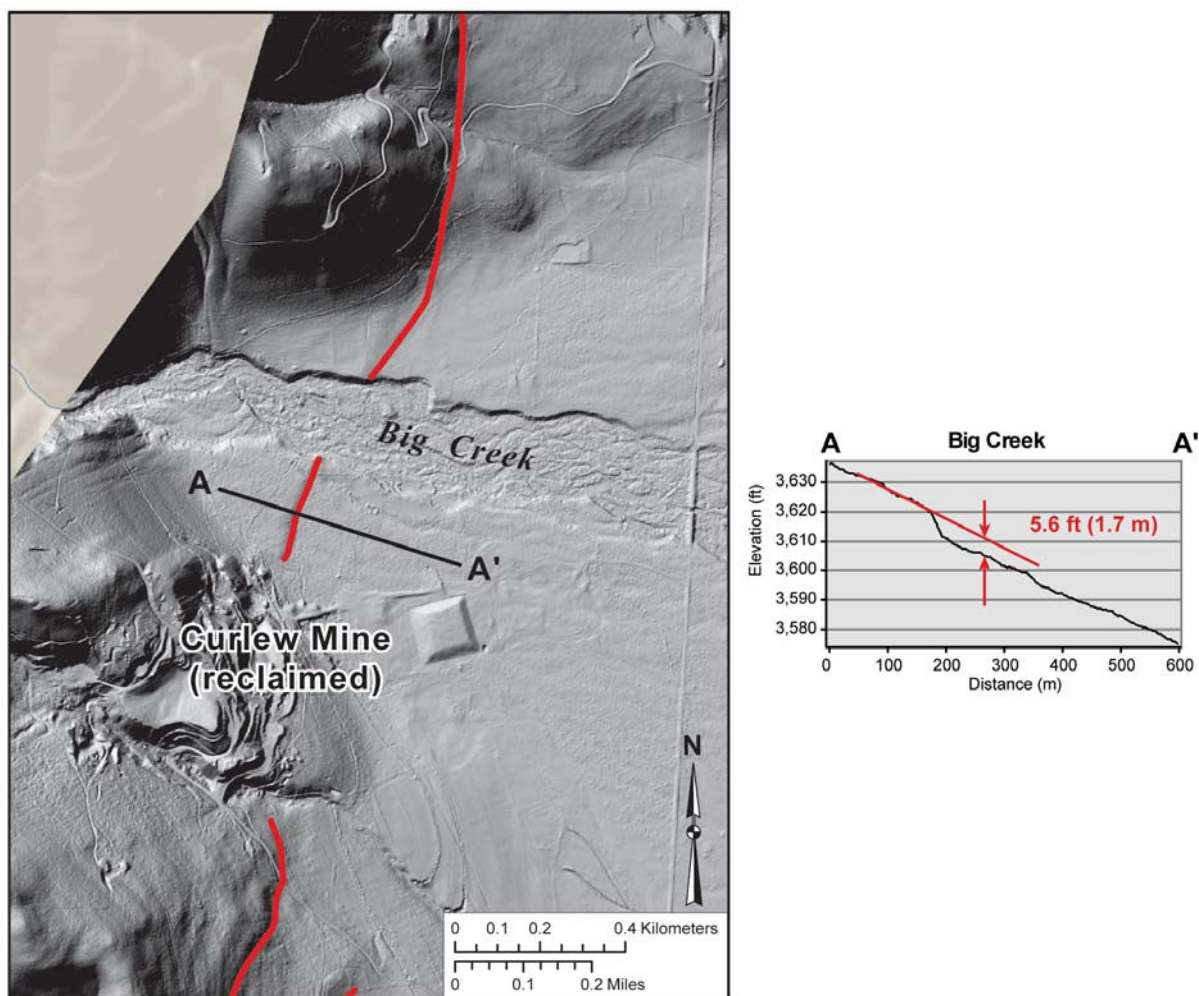

Figure 4. Topographic profile of the Big Creek scarp of the Bitterroot Fault.
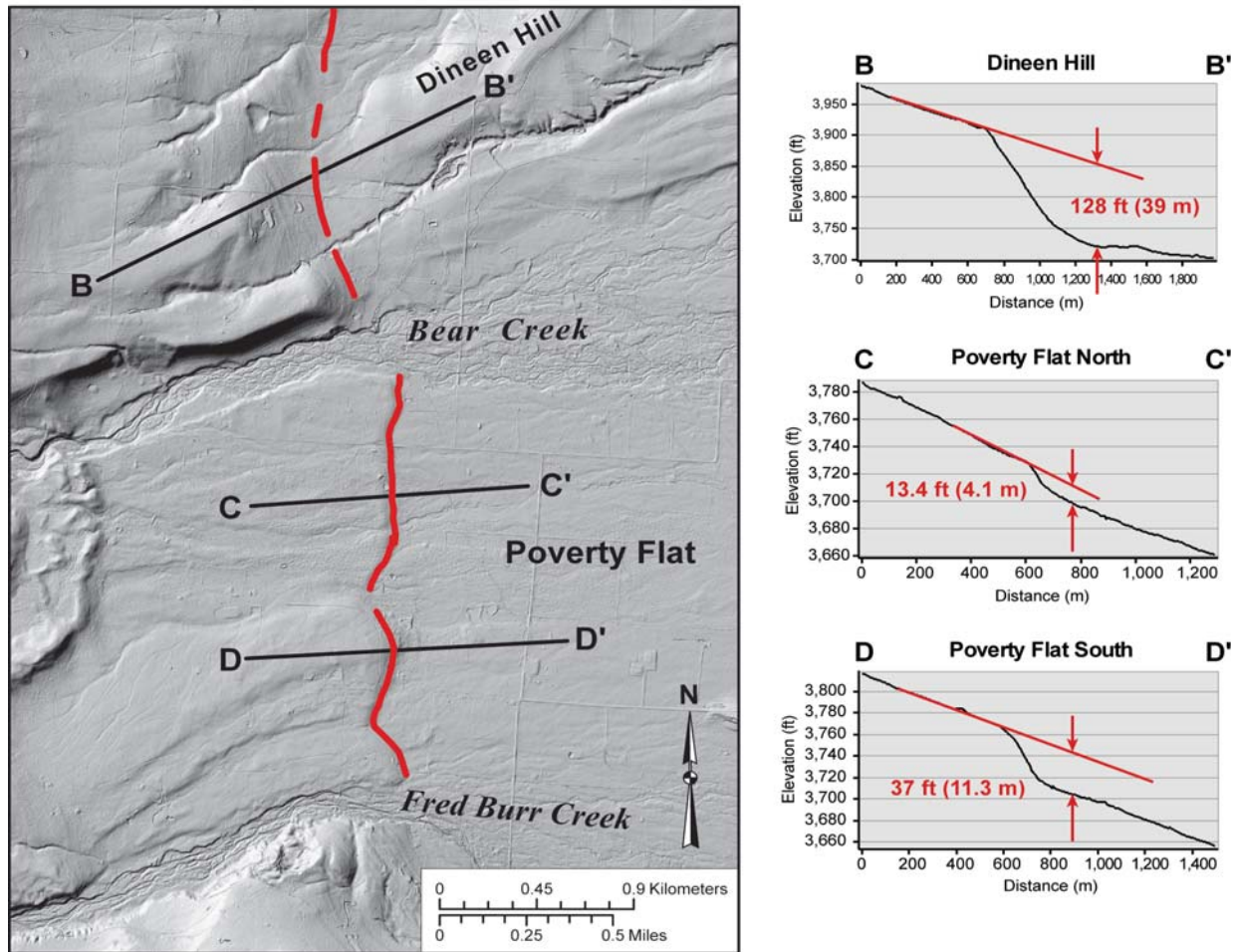
Figure 5. Topographic profiles of Bitterroot Fault scarps north of Bear Creek and on Poverty Flat.

surface is consistent with a single surface-rupturing earthquake in the latest Pleistocene or Holocene that occurred since the last glacial advance.

We generated three topographic profiles near Bear and Fred Burr Creeks (fig. 5). Tertiary-aged ancestral Bitterroot River gravels underlie profile B–B' near Dineen Hill, which shows 39 m of vertical offset as measured by projecting the uplifted footwall surface eastward above the scarp toe (fig. 5, B–B'). The pediment surface preserved on the footwall does not have a corresponding surface of the same slope on the footwall, possibly due to a long period of scarp erosion and erosional modification of the hanging wall. The gravels forming the scarp face (unit Tgc) consist primarily of well-sorted, well-rounded gravels and interbedded sand that are non-cohesive and erode easily when exposed in the scarp face. The lithological characteristics of unit Tgc result in subdued scarps with low scarp angles, despite their relatively large offsets. Our scarp height measurement represents a minimum estimate of tectonic offset of this surface, but the large scarp height clearly represents multiple surface-rup-

turing earthquakes that have occurred since the pediment surface—of unknown age—formed. Erosional strand lines of Glacial Lake Missoula mapped from the LiDAR data are visible on the on the scarp face at an elevation of 1,145 m and thus indicate that this part of the scarp existed prior to (likely much before) the last major filling of this lake. Smith and others (2018) determined that Glacial Lake Missoula initially filled to an elevation of 1,185 m by 20.9 ± 1.3 ka and last filled to this elevation prior to 13.7–13.4 ka.

Glacial outwash surfaces between Bear Creek and Fred Burr Creek are locally known as Poverty Flat. The Poverty Flat North topographic profile (fig. 5, C–C') crosses a 4.1-m scarp that cuts the low outwash terrace south of Bear Creek, mapped as unit Qgoy. The profile shows that the hanging wall surface east of the fault scarp has a slightly flatter slope than the footwall surface west of the scarp, suggesting tectonic back tilting into the scarp. The Poverty Flat terrace adjacent to Bear Creek occupies an equivalent geomorphic position to the Big Creek profile (fig. 4, A–A') located 9 km to the north and has similar surface features,

7

suggesting a post-glacial age for this surface. Based on soil development, Weber (1972) suggested that Poverty Flat formed during the early Wisconsin glaciation. The 4.1-m offset is compatible with an older surface that has experienced multiple surface-rupturing events, or alternatively if equivalent in age to the Big Creek terrace, may indicate a more active part of the Bitterroot Fault that has experienced a larger single-event offset since late Wisconsin deglaciation. A fault segment boundary between Big Creek and Bear Creek could explain such a difference in fault slip offsets.

The Poverty Flat South topographic profile (fig. 5, D–D') crosses an 11.3-m scarp on an elevated part of Poverty Flat standing up to 9 m above the elevation of the lower terrace flanking Bear Creek. We mapped this elevated surface as Qgom, an intermediate age outwash surface that we traced upstream to older glacial till deposits. The 11.3-m offset of this surface is over 2½ times greater than the offset on the lower surface just a few hundred meters to the north and is consistent with an older (early or middle Pinedale?) age for this surface. Weber (1972) mapped this elevated

part of Poverty Flat as Dutch Hill alluvium with a presumed pre-Bull Lake age. However, relict stream channels visible in the LiDAR data and relatively minor erosional dissection argue for a much younger age for this terrace surface.

South of Fred Burr Creek, along the southern edge of our northern map area, the Bitterroot Fault offsets a deeply dissected pediment surface that developed on ancestral Bitterroot River gravels (unit Tgc). A topographic profile (fig. 6, E–E') shows 43 m of offset. This large fault scarp is similar to the Dineen Hill topographic profile (fig. 5, B–B') discussed above because it has a similar vertical offset, exhibits a subdued scarp morphology because of the granular, non-cohesive deposits which it offsets, and has erosional Glacial Lake Missoula strand lines preserved on its face. As discussed in the Dineen Hill profile section above, the evidence suggests multiple surface-rupturing events have occurred along this fault since the pediment surface—of unknown age—formed.
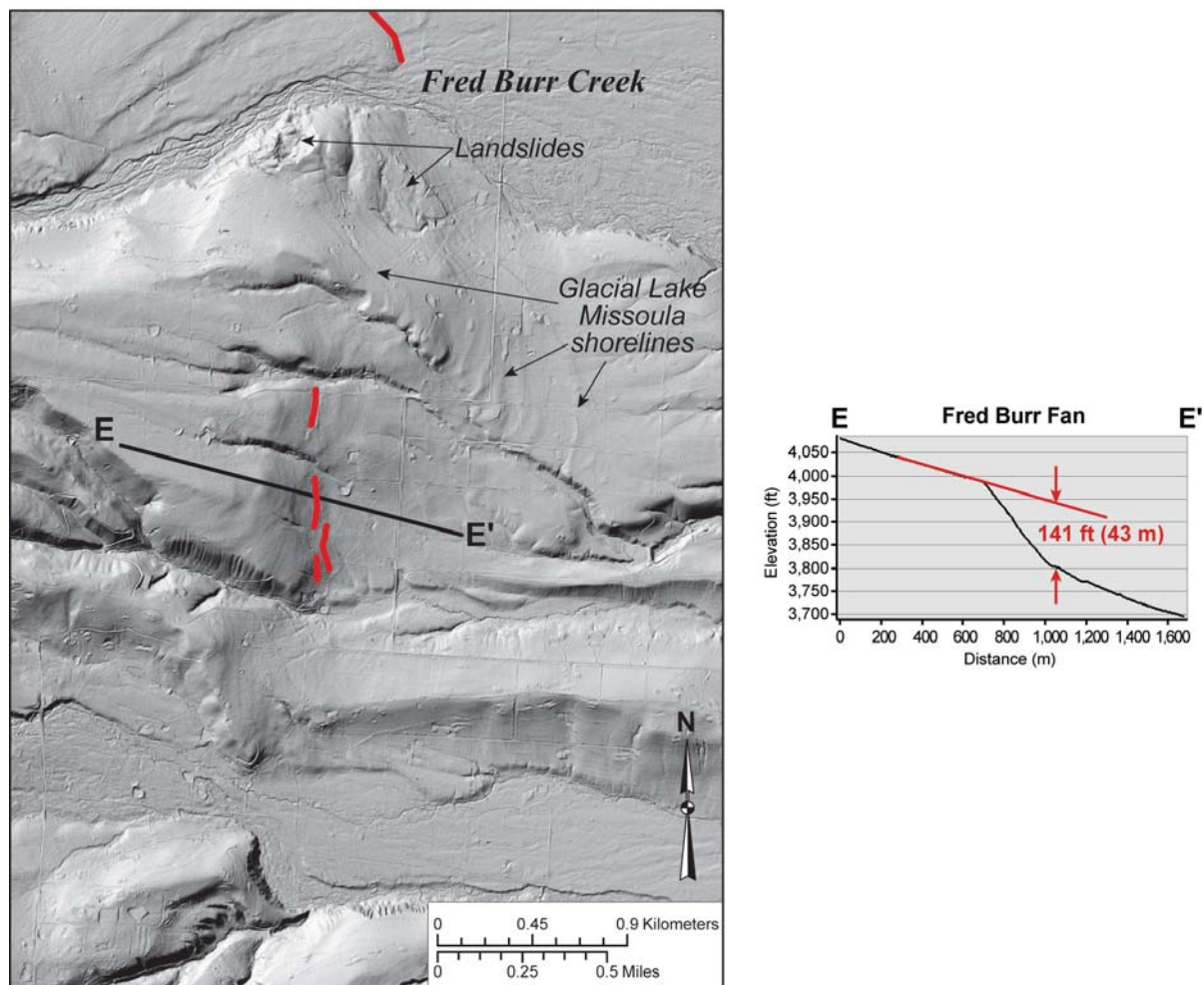

Figure 6. Topographic profile of the Bitterroot Fault scarp offsetting an alluvial fan south of Fred Burr Creek.

LIDAR ANALYSIS: FAULT OFFSET OF GEOLOGIC UNITS AND FEATURES, SOUTH BITTERROOT MAP

The Ward Creek and Lost Horse scarps are the two largest fault scarps (plate 2), possibly linked by an oblique cross-fault under modern alluvium, or alternately, en echelon features as suggested by lesser scarps that parallel the main scarps. LiDAR coverage in this area does not extend up the mountain front everywhere, and other unrecognized scarps may exist to the west.

The active trace of the Bitterroot Fault offsets the Ward Creek fan, a complex alluvial fan that formed at the base of the Bitterroot Range front below Ward Mountain (elevation 2,782 m). The Ward Creek basin is a steep, relatively small drainage basin (~2.5 km²) that supported a small Pinedale glacier, which did not extend to the range front. Ward Creek is a small perennial stream that lacks the power to transport large quantities of coarse, glacially derived sediment to the main stem of the Bitterroot River, unlike the major streams to the north and south, Roaring Lion and Lost Horse Creeks, respectively. As a result, a relatively

steep alluvial fan (sloping ~7.5° eastward below the fault scarp) accumulated at the range front, which Ward Creek and the small unnamed creek immediately to the north have dissected with channels up to 25 m deep. This dissection effectively isolated intervening northern portions of the Ward Creek fan surface from its sediment source, preserving older fan surfaces. A narrow channel about 25 m wide and 3 m deep incises the more aerially extensive central part of the Ward Creek fan and is filled with very coarse boulder and cobbles, which widens and bifurcates below the fault scarp. We interpret this shallow channel filled with very coarse sediment as a young debris flow deposit that constitutes the youngest part of the Ward Creek alluvial fan surface. We constructed topographic profiles across the fault scarp where it offsets four distinct surfaces of the Ward Creek fan (fig. 7).

The oldest part of the Ward Creek alluvial fan is preserved between the incised modern channels of Ward Creek and a small unnamed creek to the north. A topographic profile crossing the fault cutting this fan surface remnant indicates a vertical scarp height of 14 m (fig. 7, F–F'). This topographic profile and our field examination of this site (fig. 8) suggest that the hang-
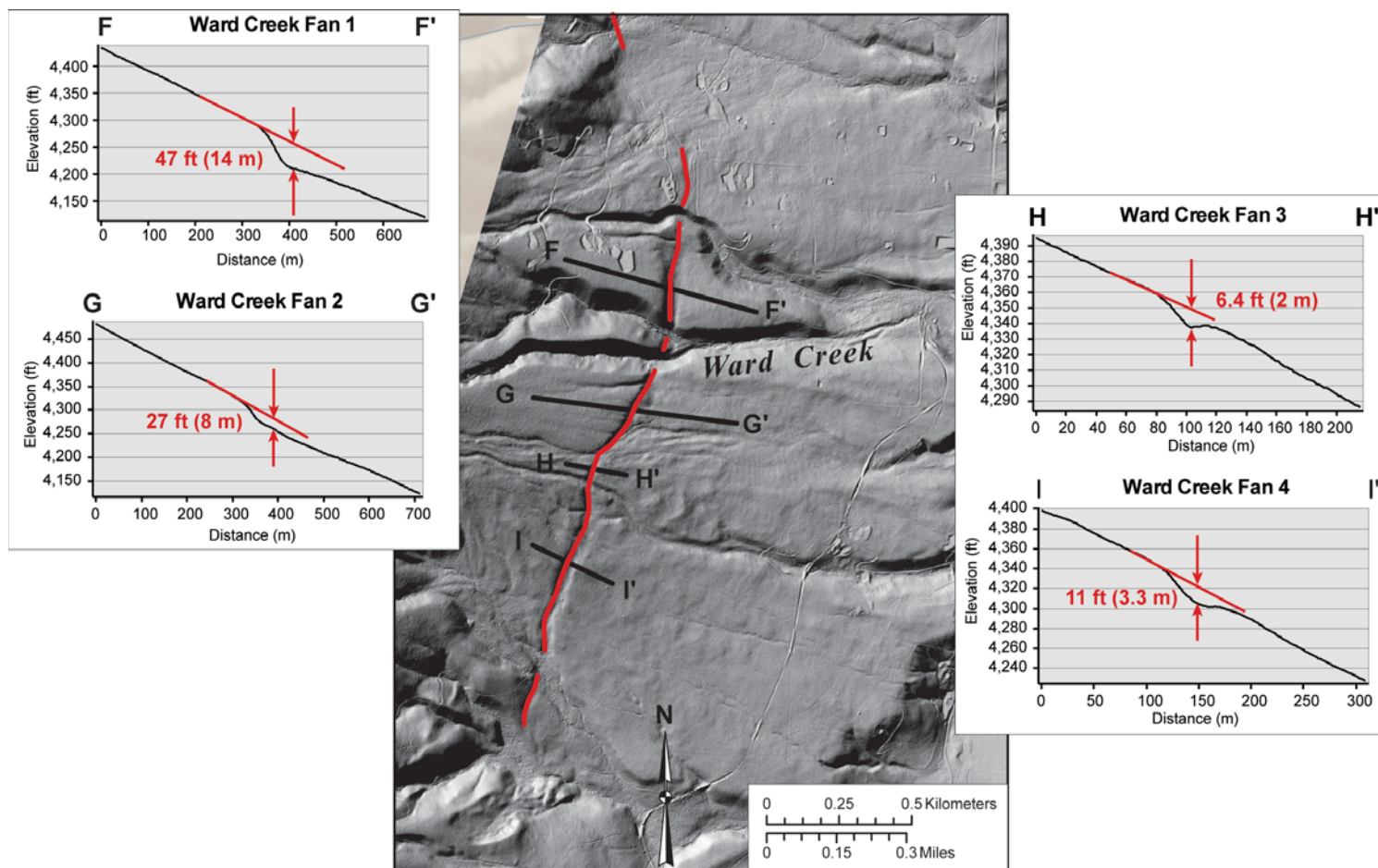

Figure 7. Topographic profiles of the Bitterroot Fault scarp offsetting different aged parts of the Ward Creek fan.

Figure 8. Northwestward view of the Bitterroot Fault offsetting the oldest surface on the Ward Creek alluvial fan near topographic profile F–F' shown in figure 7. Note the slight back tilting of the hanging block surface on the right into the base of the fault scarp.

ing wall block just below the fault has experienced back tilting and minor graben formation along a small antithetic fault, so this scarp height measurement probably overestimates net vertical tectonic displacement. A conservative estimate of net vertical tectonic displacement is at least 10–12 m.

A topographic profile constructed about 200 m south of Ward Creek reveals 8 m of surface offset of the Ward Creek alluvial fan surface (fig. 7, G–G'). This part of the fan has a smooth surface lacking the obvious hummocky morphology that is apparent on the fan surfaces to the south. This smooth surface character, together with the presence of a 250-m-long gully incised into the upthrown footwall block, suggest that this part of the fan surface is older than areas to the south. Although it is not obvious from the topographic profile, a small graben visible in the LiDAR data and on the ground parallels the main fault scarp. The parallel orientation of fan surfaces above and below the fault in this profile suggests that the vertical surface offset measured is a reasonable estimate of net tectonic displacement on this surface.

We constructed a topographic profile along the shallow debris flow channel (unit Qgdy) where it

crosses the fault (fig. 7, H–H'). This profile, which is about one-third as long as the previous two profiles discussed above, clearly shows a graben at the toe of the fault scarp. Measured from the profile downslope of the graben, we find a surface offset of 2 m. We believe that the bouldery deposits filling this channel, set into the surround fan surface and exhibiting hummocky surface morphology below the fault scarp, represent the youngest Pinedale deposit composing the Ward Creek alluvial fan.

The most aerially extensive part of the Ward Creek fan lies south of the debris flow channel discussed above. We constructed a topographic profile across this fan surface and measured 3.3 m of surface offset (fig. 7, I–I'). A graben is readily apparent in both the topographic profile and the LiDAR imagery. We measured the surface offset downslope of the graben. The LiDAR imagery shows muted hummocky topography and minimal dissection of the footwall block, suggesting that this surface is younger than the surfaces profiled in figure 7, F–F' and G–G', even though we mapped all three of these surfaces as unit Qgdo (older glacial debris flow deposits). The significant range of scarp height/surface offset measurements (profiles/

10

offsets: F–F'/14 m; G–G'/8 m; and I–I'/ 3.3 m) on three parts of the Ward Creek fan mapped as the same unit within 1 km of each other suggests repeated surface ruptures across fan surfaces with different ages.

We constructed a topographic profile across the Bitterroot Fault on a glacial outwash terrace (unit Qgoy) south of Camas Creek (fig. 9, J–J') that shows 2.4 m of surface offset. This geomorphic surface and amount of offset is similar to the Big Creek profile (fig. 4, A–A') and may represent the most recent surface faulting event.

We constructed a topographic profile across the Bitterroot Fault where it offsets ancestral Bitterroot gravels (unit Tcg) just north of the North Fork of Hayes Creek (fig. 9, K–K'). The profile indicates a scarp height of 10.8 m. A well-dissected pediment surface developed on the ancestral Bitterroot gravels forms the footwall block surface of the fault in this area. Similar to other areas where the scarp cuts these non-cohesive gravels, the scarp morphology is subdued and indistinct.

We constructed our southernmost topographic profile just north of Lost Horse Creek (fig. 9, L–L') that shows 6 m of surface offset in older glacial till deposits (unit Qgto). The planar nature of these deposits along a topographic low, which parallels the channels of Hayes Creek to the north and Lost Horse Creek to the south, suggests that this topographic profile may follow an abandoned stream channel incised into old glacial till. This profile is just down canyon beyond the furthest extent of the youngest glacial moraine (unit Qgty), which we presume to be latest Pinedale.

DISCUSSION

We have estimated relative ages of mapped Quaternary deposits based on stratigraphic and geomorphic relations, but have no absolute age control for these units or the geomorphic surfaces developed upon them. Lacking age control, we have reviewed the glacial histories from other, well-studied mountain ranges in the surrounding region. The climate of the Bitterroot Mountains has a stronger maritime influence than
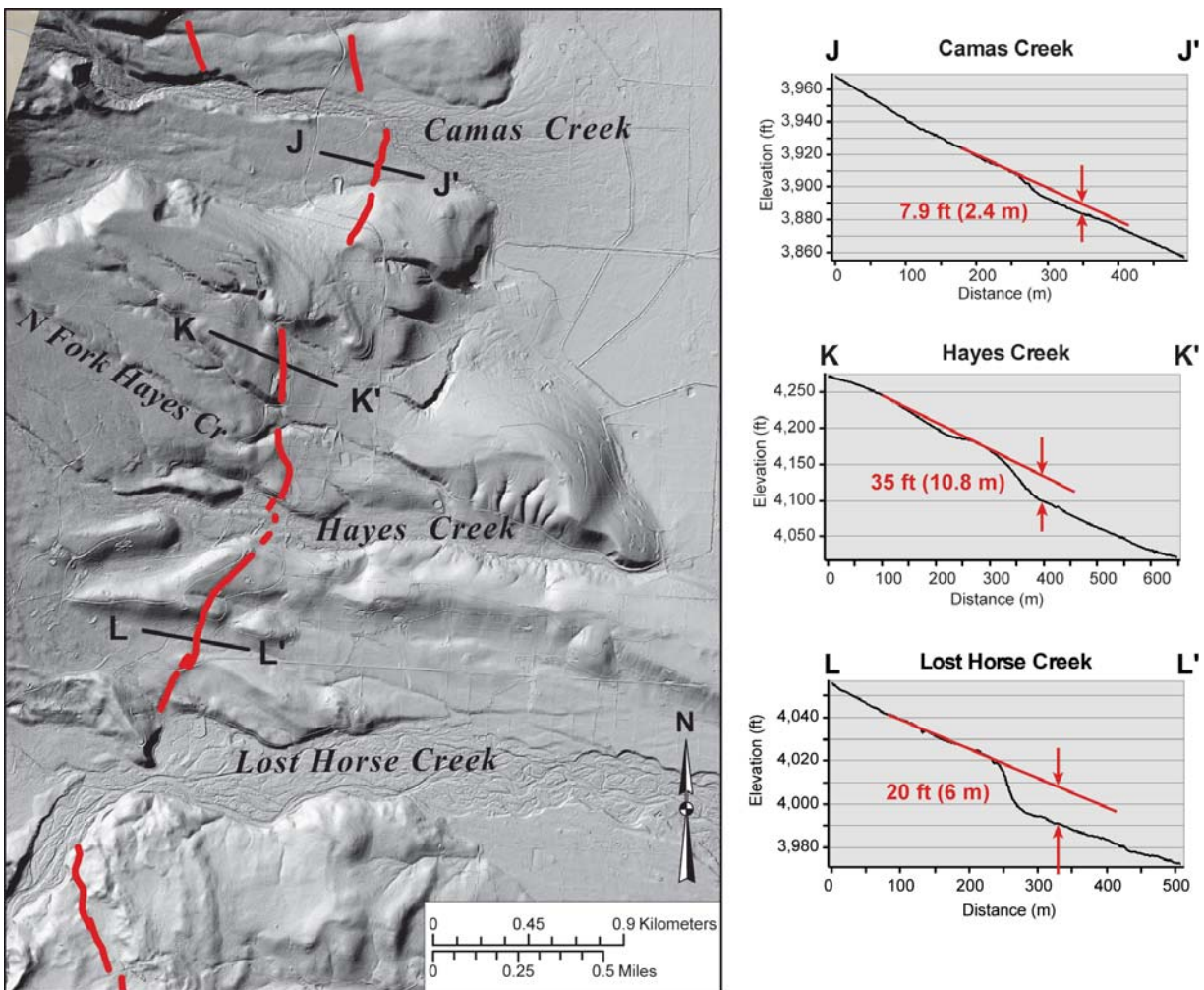

Figure 9. Topographic profiles of the Bitterroot Fault scarp in the Camas Creek–Lost Horse Creek area.

most intermountain west ranges (PRISM climate data), and its glacial history is probably similar to the well-studied Wallowa, Teton, and Sawtooth Ranges (Thackray, 2008; Thackray and others, 2013; Pierce and others, 2018). In the Wallowa and Sawtooth Ranges, the most recent glacial advances beyond the range front ended 11–12 ka (Thackray, 2008; Thackray and others, 2013), while in the Tetons, deglaciation occurred about 14 ka (Thackray and Staley, 2017; Pierce and others, 2018). Therefore, we suggest that the younger till and outwash (units Qgty, Qgoy, Qgdy) that are consistently offset by the fault scarps are about 11–14 ka. The observation that no Glacial Lake Missoula strand lines are visible on these deposits, and Lake Missoula's last stand was at 12.2–12.5 ka (Hanson and Clague, 2016) and prior to 13.7–13.4 ka (Smith and others, 2018), lends support to this speculation.

Surface offsets in post-glacial outwash terraces flanking Big Creek (1.7 m), Poverty Flat (4.1 m), and Camas Creek (2.4 m) are consistent with slip rates in the 0.1 to 0.3 m/ka range. This range of slip rates is in line with other range-front normal faults in Montana (Stickney and others, 2000), but lacking age control for the faulted deposits, our estimates at this point are speculative.

The ages of the older and more extensive glacial deposits (Qgoo, Qgdo, Qgom, Qgto) are even more poorly known. They could be as young as the 20–23 ka maximum advances in the Sawtooth and Wallowa Ranges, or as old as the 72 ka maximum in the Cascades (Thackray, 2008), or somewhere between as in the 16–45 ka glacial advances of the Tetons (Thackray and Staley, 2017). Possibly the "middle-aged" outwash (Qgom) represents a 20–23 ka advance and the older glacial deposits resulted from a 45–72 ka maximum. Because both we and Weber (1972) observed that boulders in the older deposits are noticeably more weathered than those in the younger deposits, we postulate that Qgom represents 45 ka outwash, and that Qgoo may be as old as 72 ka.

The pediment surface developed on Miocene (?) Tgc has a minimum age only constrained by the age of these older glacial deposits that were deposited on it. Obviously our future understanding of the Bitterroot Fault will depend greatly on obtaining age data to constrain the offsets.

However, even lacking dates for the mapped Qua-ternary deposits and surfaces, the significantly greater offsets in older deposits demonstrate repeated surface-rupturing earthquakes. The magnitudes of these prehistoric earthquakes are unknown but must have been at least magnitude 6.5 (dePolo, 1994). Earthquake magnitudes depend mainly on fault surface rupture area (length x width) and amount of slip. The ~100-km length of the Bitterroot Fault is certainly long enough to be composed of two or three segments that may rupture independently of each other. The question of fault segmentation cannot be answered without offset histories (usually determined by trenching) at multiple sites along the fault. A scenario earthquake, in which the entire 100-km length of the Bitterroot Fault is assumed to slip 2 m, suggests a magnitude of 7.2 (U.S. Geological Survey Montana Earthquake Scenario Catalog), resulting in extensive damage and economic impacts (Earthquake Engineering Research Institute).

ACKNOWLEDGMENTS

DESCRIPTION OF MAP UNITS

md—**Man-made disturbance (Holocene)**—Area around the Curlew Mine and subsequent reclamation activites.

Qal—**Stream alluvium (Holocene and Late Pleistocene)**—Subangular to rounded, moderately to well sorted and stratified, pebble to boulder sandy gravel. Gravel clasts representative of drainage basins. Includes floodplain areas of sand, silt, and clay. Primarily quartzite, siltite, and volcanic rocks. Includes minor colluvium, fan deposits, and pebbly to cobbly sandy silt in local lower energy drainages. Deposits are 1–18 m (3–60 ft) thick, and average 12 m (40 ft) (McMurtrey and others, 1972).

Qaf—**Small alluvial fan and debris-flow deposits (Holocene and Late Pleistocene)**—Sub-angular to rounded, poorly sorted, matrix-supported pebble to boulder gravel in a sand, silt, and clay matrix. Commonly grades into, interfingers with, and caps stream alluvium (Qal). Thickness varies greatly, ranging from 1 to 24 m.

Qafo—**Older alluvial fan and debris flow deposits (Pleistocene)**—Sub-angular to rounded, moderately to poorly sorted pebble to boulder gravel in a sand, silt, and clay matrix. Clasts locally derived. Thickness less than 20 m.

Qls—**Landslide and earthflow deposits (Holocene and late Pleistocene)**—Unsorted and unstratified mixtures of locally derived material transported down adjacent steep slopes and characterized by irregular hummocky surfaces. Occurs most commonly as earthflows on slopes underlain by clay-rich facies of the ancestral Bitterroot River deposits (Tgc).

Qpa—**Paludal deposit (Holocene)**—Sand, silt, clay, and organic matter deposited in swamp, marsh, pond, or lake. Thickness probably less than 10 m (33 ft).

Qatr—**Alluvium of the Riverside Terrace (late Pleistocene?)**—Well-rounded, well-sorted gravel and sand underlying the youngest terrace, termed the Riverside terrace by Weber (1972), along the Bitterroot River. The surfaces of these deposits stand 10 to 15 ft above the present floodplain. Thickness estimated at 10 to 20 ft. Predominantly granitic, gneissic, and Belt quartzite and argillite clasts derived from the Belt Supergroup, with minor volcanic clasts.

Qath—**Alluvium of the Hamilton Terrace (late Pleistocene?)**—Well-rounded, well-sorted gravel and sand underlying the second youngest terrace, the Hamilton terrace (Weber, 1972), along the Bitterroot River. The surfaces of these deposits stand 20 to 25 ft above the present floodplain. Thickness is from 10 to 30 ft. Predominantly granitic, gneissic, and Belt sedimentary clasts, with minor volcanic clasts.

Qgoy—**Younger glacial outwash deposits (late Pleistocene)**—Subrounded to well-rounded, moderately sorted, unweathered cobbles and boulders in a matrix of sand and gravel deposited in outwash fans downstream from Pinedale-age glaciers. Surfaces of these deposits are at a lower level than older outwash (Qgoo and Qgom). Can be traced upstream to glacial till deposits of Pinedale age (Qgty). Surfaces of these deposits stand 5–25 ft above the active channels. Some fans appear to coalesce with alluvial terrace deposits (Qatr and Qath). Thickness averages 12 m (McMurtrey and others, 1972).

Qgdy—**Younger glacial debris flow deposits (late Pleistocene)**—Subangular to well-rounded, poorly sorted, matrix-supported, unweathered boulders and cobbles in a matrix of sand, gravel, and clay. Characterized by boulders as much as 3 m in diameter, and by a hummocky appearance on the Lidar image. Deposited in debris-flow fans below Pinedale-age glaciers, probably as a result of catastrophic glacial outburst floods. Thickness probably 2–12 m.

Qgom—**Middle-aged glacial outwash deposits (Pleistocene)**—Subrounded to well-rounded, moderately sorted, unweathered cobbles and boulders in a matrix of sand and gravel deposited in outwash fans downstream from Pleistocene glaciers. Surfaces of these deposits stand at an intermediate level between younger and older glacial outwash (Qgoy and Qgoo), but their absolute ages are unknown. They can be traced upstream to older glacial till deposits (Qgto). Thickness probably 6–12 m.

Qgdm—**Middle-aged glacial debris flow deposits (late Pleistocene)**—Subangular to well-rounded, poorly sorted, matrix-supported, unweathered boulders and cobbles in a matrix of sand, gravel, and clay. Characterized by boulders as much as 3 m in diameter, and by a hummocky appearance on the Lidar image. Surfaces of these deposits stand at an intermediate level between younger and older glacial outwash (Qgoy and Qgoo), but their absolute ages are unknown. Deposited in debris-flow fans, probably as a result of catastrophic glacial outburst floods. Thickness probably 2–12 m.

Qgoo—**Older glacial outwash deposits (Pleistocene)**—Subrounded to well-rounded, moderately sorted, variably weathered cobbles and boulders in a matrix of sand and gravel deposited in outwash fans downstream from Pleistocene glaciers. Surfaces of these deposits lie above the younger outwash fans (Qgoy and Qgom), and they typically mantle pediments developed on the ancestral Bitterroot River deposits (Tgc). Mapped as Tertiary Sixmile Creek Formation on Lonn and Sears (2001), but reassigned to a Pleistocene age herein because they can be traced upstream to older glacial moraines (Ogto). Thickness from 2–12 m.

Qgdo—**Older glacial debris flow deposits (Pleistocene)**—Subangular to well-rounded, poorly sorted, matrix-supported, variably weathered boulders and cobbles in a matrix of sand, gravel, and clay. Characterized by boulders as much as 3 m in diameter, and by a slightly hummocky appearance on the Lidar image. Deposited in debris-flow fans below Pleistocene glaciers, probably as a result of catastrophic glacial outburst floods. Typically mantle pediments developed on the ancestral Bitterroot River deposits (Tgc). Mapped as Tertiary Sixmile Creek Formation on Lonn and Sears (2001), but reassigned to a Pleistocene age herein because they can be traced upstream to older glacial moraines (Qgto). Thickness ranges from 12 m at the heads of fans to less than 2 m near the toes.

Qgty—**Younger glacial till deposits (late Pleistocene)**—Unsorted, mostly unstratified, clay, silt, sand, and gravel containing boulders up to 6 m in diameter. Clasts subangular to subrounded and unweathered. Deposited in Pinedale-age glacial moraines typically inset within older moraines (Qgto). Characterized by very hummocky appearance on the Lidar image. Thickness probably ranges from 10 to 120 m.

Qgto—**Older glacial till deposits (Pleistocene)**—Unsorted, mostly unstratified, clay, silt, sand, and gravel containing boulders up to 6 m in diameter. Clasts subangular to subrounded and variably weathered. Deposited in Pleistocene glacial moraines. Characterized by their smooth surfaces on the Lidar image in contrast to younger till (Qgty) with well-preserved hummocky topography. Weber (1972) postulated that at least two different glacial stages are represented by these deposits, but we could not distinguish them in the field or on the Lidar image. Thickness ranges from 10 to 120 m.

Tgc—**Gravel and clay of the ancestral Bitterroot River deposits (Oligocene to Pliocene?)**—Unconsolidated, well-sorted, stratified, well-rounded, fluvial gravel and sand interbedded with light tan clay, silt, and tephra. Deposited in channels and floodplains of the ancestral Bitterroot River (Lonn and Sears, 2001). Gravel deposits contain well-rounded cobbles and pebbles of (in order of decreasing abundance): Belt quartzite, granite/granodiorite, mylonitic gneiss, high-grade metamorphic rocks, and extrusive volcanic rocks that represent rocks exposed in the entire Bitterroot River drainage. Interbedded finer grained deposits, probably deposited in adjacent floodplains, are light gray clay and silt deposits in beds 6 in to 5 ft thick, with abundant interbedded tephra. Some brown, ledge-forming massive silty layers with root casts and burrows are present and interpreted to be paleosols. Fossil assemblages collected by Konizeski (1958) and McMurtrey and others (1972) ranged from Oligocene to late Miocene in age, and a recently unearthed fossil was estimated to be 7–9 Ma (Dale Hanson, Museum of the Rockies, written commun., 2018). Deep drill holes show that unconsolidated sedimentary rocks similar to Tgc are up to 700 m thick (Norbeck, 1980). Unit Tgc also occurs 450 m above the valley floor along the Bitterroot Mountain front in the northern Bitterroot map area, where it is interpreted to have been elevated to this position by faults. Lower contact is exposed in two places on the southern Bitterroot map where Tgc unconformably overlies brecciated granitic bedrock. Upper contact is an erosional (pediment) surface with a minimum age constrained by the overlying Pleistocene glacial outwash deposits.

Tgcd—**Debris flow deposits that grade into Tgc (Oligocene to Pliocene?)**—Poorly sorted angular quartzite cobbles, pebbles present adjacent to the Bitterroot Mountain front that grade laterally into Tgc gravel and clay deposits 2 km southwest of the Curlew Mine in the northern Bitterroot map area, and well-rounded quartzite boulders and cobbles of the fluvial facies of the ancestral Bitterroot deposits overlie Tgcd. In other places, the two facies appear to interfinger. Tgcd overlies brecciated quartzite and calc–silicate bedrock of the Bitterroot detachment hanging wall, and is interpreted to represent debris flow deposits eroded from the hanging wall. The debris flow deposits are postulated to interfinger with and grade laterally into fluvial facies Tgc towards the center of the valley.

TKg—**Foliated granodiorite and unfoliated granite, undivided (Cretaceous and Eocene)**—In the footwall of the Bitterroot detachment, unit is weakly foliated to gneissic Cretaceous to Eocene biotite–muscovite granodiorite intruded by unfoliated Eocene biotite–muscovite granite. Fabrics in the granodiorite developed at deep levels early in the Bitterroot detachment Fault's history, while the Eocene granite intruded at shallow levels following most of the plastic deformation. In the B-detachment hanging wall, both unfoliated Eocene biotite–muscovite granite and weakly foliated to unfoliated biotite–muscovite granodiorite occur. Unit also includes outcrop-scale inclusions of Belt Supergroup metasedimentary rock that are too small to show on the map. A thick brecciated zone occurs along the B-detachment Fault, and is marked by breccia symbols on the maps.

TYsc—**Belt metasedimentary rocks, granodiorite, and granite, undivided (Mesoproterozoic, Cretaceous, and Eocene)**—Quartzite, calc–silicate gneiss of the Belt Supergroup and Cretaceous to Eocene granodiorite and granite. All have been severely brecciated, and are interpreted to represent hanging wall rocks preserved immediately above the Bitterroot detachment Fault.

Ys—**Belt metasedimentary rocks (Mesoproterozoic)**—Brecciated quartzite and calc–silicate gneiss of the Belt Supergroup exposed along the Bitterroot Mountain front. Similar lithologies are found unbrecciated in the Sapphire Mountains to the east in the hanging wall of the Bitterroot detachment, and so these rocks are thought to represent pieces of the hanging wall preserved in the Bitterroot Mountain foothills.

Xm—**Metamorphic rocks (Paleoproterozoic)**—Quartzite, amphibolite, and calc–silicate gneiss continuous with the postulated basement rocks of Sleeping Child Creek in the Sapphire Mountains (west of the map areas shown in plate 2) in the hanging wall of the Bitterroot detachment. A U–Pb crystallization age of 1,860 Ma was obtained for the Sleeping Child orthogneiss (Jesse Mosolf, MBMG, written commun., 2016) just east of the southern map area.

REFERENCES CITED

Barkman, P .E., 1984, A reconnaissance investigation of active tectonism in the Bitterroot Valley, western Montana: Missoula, University of Montana, M.S. thesis, 85 p.

Berg, R.B., and Lonn, J.D., 1996, Preliminary geologic map of the Nez Perce Pass 30 x 60 minute quadrangle, Montana: Montana Bureau of Mines and Geology Open-File Report 339, scale 1:100,000.

Cartier, K.D.W., 1984, Sediment, channel morphology, and streamflow characteristics of the Bitterroot River drainage basin, southwestern Montana: Missoula, University of Montana, M.S. thesis, 191 p.

dePolo, C.M., 1994, The maximum background earthquake for the Basin and Range Province, western North America: Bulletin of the Seismological Society of America, v. 84, p. 466–472.

Earthquake Engineering Research Institute, Montana Earthquake Scenarios, http://www.nehrpscenario.org/completed/montana-earthquake-scenarios/ [Accessed 5/11/2018].

Foster, D.A., and Raza, A., 2002, Low-temperature thermochronological record of exhumation of the Bitterroot metamorphic core complex, northern Cordilleran Orogen: Tectonophysics, v. 349, p. 23–36.

Foster, D.A., Schaferb, C., Fanning, C.M., and Hyndman, D.W., 2001, Relationships between crustal partial melting, plutonism, orogeny, and exhumation: Idaho–Bitterroot batholith: Tectonophysics, v. 342, p. 313–350.

Hanson, M.A., and Clague, J.J., 2016, Record of glacial Lake Missoula floods in glacial Lake Columbia, Washington: Quaternary Science Reviews, v. 133, p. 62–76.

Hanson, M.A., Lian, O.B., and Clague, J.J., 2012, The sequence and timing of large late Pleistocene floods from glacial Lake Missoula: Quaternary Science Review, v. 31, p. 67–81, http://dx.doi.org/10.1016/j.quascirev.2011.11.009.

Hunter, L.E., Howle, J.F., Rose, R.S., and Bawden, G.W., 2011, LiDAR-assisted identification of an active fault near Truckee, California: Bulletin of the Seismological Society of America, v. 101, no. 3, p. 1162–1181, doi: 10.1785/0120090261 [Accessed 6/16/2018].

Hyndman, D.W., 1980, Bitterroot dome–Sapphire tectonic block, an example of a plutonic core–gneiss–dome complex with its detached suprastructure, in Crittenden, M.D., Coney, P.J., and Davis, G.H., eds., Cordilleran Metamorphic Core Complexes: Geological Society of America Memoir, v. 153, p. 427–443.

Konizeski, R.L., 1958, Pliocene vertebrate fauna from the Bitterroot Valley, Montana, and its stratigraphic significance: Geological Society of America Bulletin 69, p. 325–345.

Lageson, D.R., and Stickney, M.C., 2000, Seismotectonics of northwest Montana, USA: Montana Geological Society 50th Anniversary Symposium, Montana/Alberta Thrust Belt and Adjacent Foreland, R.A. Schalla and E.H. Johnson, eds., v. 1, p. 109–126.

Lonn, J.D., and Berg, R.B., 1996, Preliminary geologic map of the Hamilton 30 x 60 minute quadrangle, Montana: Montana Bureau of Mines and Geology Open-File Report 340, scale 1:100,000.

Lonn, J.D., and Sears, J.W., 2001, Geology of the Bitterroot Valley, shaded relief: Montana Bureau of Mines and Geology Open-File Report 441-C, 1 sheet, scale 1:48,000.

McMurtrey, R.G., Konizeski, R.L., Johnson, M.V., and Bartells, J.H., 1972, Geology and water resources of the Bitterroot Valley, southwestern Montana: U.S. Geological Survey Water Supply Paper 1889, 80 p., scale 1:125,000.

Norbeck, P.M., 1980, Preliminary evaluation of deep aquifers in the Bitterroot and Missoula valleys in western Montana: Montana Bureau of Mines and Geology Open-File Report 46, 15 p.

Pierce, K.L., Licciardi, J.M., Good, J.M., and Jaworowski, C., 2018, Pleistocene glaciation of the Jackson Hole area, Wyoming: U.S. Geological Survey Professional Paper 1835, 56 p., doi.org/10.3133/pp1835.

PRISM climate data, NOAA Research, https://www.esrl.noaa.gov/psd/data/gridded/data.prism.html [Accessed 5/11/2018].

Ross, C.P., 1952, The eastern front of the Bitterroot Range, Montana: U.S. Geological Survey Bulletin 974, p. 135–175, scale 1:125,000.

Smith, L.N., Sohbati, R., Buylaert, J.P., Lian, O.B., Murry, A., and Jain, M., 2018, Time of lake-level changes for a deep last-glacial Lake Missoula: Optical dating of the Garden Gulch area, Montana, USA: Quaternary Science Reviews, p. 23–35, doi 10.1016/j.quascirev.2018.01.009.

Stickney, M.C., and Bartholomew, M.J., 1987, Seismicity and late Quaternary faulting of the northern Basin and Range Province, Montana and Idaho: Bulletin of the Seismological Society of America, v. 77, p. 1602–1625.

Stickney, M.C., Haller, K.M., and Machette, M.N., 2000, Quaternary faults and seismicity in western Montana: Montana Bureau of Mines and Geology Special Publication 114, scale 1:750,000.

Thackray, G.D., 2008, Varied climatic and topographic influences on Late Pleistocene mountain glaciation in the western United States: Journal of Quaternary Science, v. 23, no. 6–7, p. 671–681.

Thackray, G.D., Rodgers, D.W., and Streutker, D., 2013, Holocene scarp on the Sawtooth fault, central Idaho, USA, documented through lidar topographic analysis: Geology v. 41, no. 6, p. 639–642, doi:10.1130/G34095.1.

Thackray, G.D., and Staley, A.E., 2017, Systematic variation of Late Pleistocene fault scarp height in the Teton Range, Wyoming, USA: Variable fault slip rates or variable landform ages?: Geosphere, v. 13, no. 2, p. 287–300, doi:10.1130/GES01320.1.

Toth, M.I., 1983, Reconnaissance geologic map of the Selway–Bitterroot Wilderness, Idaho County, Idaho, and Missoula and Ravalli Counties, Montana: U.S. Geological Survey Miscellaneous Field Studies Map MF-1495-B, scale 1:125,000.

U.S. Geological Survey and Montana Bureau of Mines and Geology, 2006, Quaternary fault and fold database for the United States, https://earthquake.usgs.gov/hazards/qfaults/citation.php [Accessed 6/15/2018].

U.S. Geological Survey Montana Earthquake Scenario Catalog, https://earthquake.usgs.gov/scenarios/catalog/mt2016/ [Accessed 5/11/2018].

Weber, W.M., 1972, Correlation of Pleistocene glaciation in the Bitterroot Range, Montana, with fluctuations of glacial Lake Missoula: Montana Bureau of Mines and Geology Memoir 42, 42 p.